Current Topics in Electrochemistry
Vol. 24, 2022

Original Article

Modeling deposition of metal and energy fluxes during TaN and TiN sputtering

Junqing Lu*

Advanced Materials Engineering, Keimyung University, 1095 Dalgubeol Road, Daegu, 42601, South Korea.

ABSTRACT

The reactive sputtering processes are used to deposit metal nitride films (TiN and TaN) with superior material properties. This study investigates the fluxes and the associated energies of the sputtered metal atoms (Ti and Ta), the reflected energetic Ar atoms, and the ions (Ar^+ and N_2^+) to the substrate. A collisionless transport model based on thermal flux analogy was used to calculate the atom fluxes to the substrate. The results from previous studies were used to calculate the energy levels of the neutral atoms. The ion densities from a previous study and a sheath energy model were used for the ion energy and fluxes. The calculated values indicate that the energy levels for both atoms and ions are elevated during the sputtering process, and the ion energy levels (above 60 eV) are higher than the energy level of the neutrals by about 20 to 30 eV. In addition, the total ion flux to the substrate is about 10 times the neutral flux. Consequently, the total ion energy flux to the substrate is dominant (25 to 50 times) over the total neutral energy flux.

KEYWORDS: plasma nitriding, sputter, metal flux, energy flux.

1. INTRODUCTION

Metal nitride films such as TiN and TaN are extensively used in electronics and metallurgy as diffusion barriers and protective coatings [1-3]. These metal nitride films could be formed using various processing methods. The reactive sputtering method is often preferred because this method can produce superior electrical and mechanical film properties [4-6]. For example, the hardness and resistivity of the TiN thin film could be optimized by applying -300 V bias at the substrate during the deposition process [4].

It has been recognized that the energetic particles generated during the sputter process are responsible for the improved thin film properties. Hence, efforts were directed to investigate these energetic particles. Due to the difficulties in measuring the plasma particle energy directly through experimental methods, modeling methods were often used. For example, a Monte Carlo model was used to predict the power inputs by the energetic particles to the sputter cathode and the subsequent gas heating effect for Cu ad Al depositions [7]. Another Monte Carlo model was used to predict the deposition rate of the sputtered atoms onto the substrate [8]. A hybrid Monte Carlo and fluid model was used to study the Al sputter, and the depositing Al species fluxes to the substrate were computed [9].

A previous modeling study indicates that the energetic particles in the plasma could contribute to a large amount of energy during the metal nitride film deposition process, thereby improving the film properties [10]. For the reactive sputtering of metal nitrides, the sputter target is

*Email id: junqinglu@yahoo.com

usually pure metal, and a mixture of Ar and N_2 gas is used to form the plasma. The Ar ions in the plasma sputter the metal atoms from the target. The sputtered metal atoms deposit onto the substrate, and form metal nitride on the substrate through surface reactions.

At low pressure conditions, there are more energetic particles incident onto the substrate because these energetic particles have few thermalizing collisions with the background gas atoms or molecules. There are three types of energetic particles arriving at the substrate. The first is the sputtered metal atoms, which are emitted from the target with a Thompson energy distribution [7] and consequently have a relatively high average energy. The second is the reflected Ar neutrals. After the incident Ar^+ ions hit the target surface, these Ar^+ ions are neutralized and reemitted from the target as Ar atoms (neutrals). These reemitted Ar atoms are also called reflected Ar neutrals, which have much higher energy than the regular Ar atoms in the plasma. Some of the reflected Ar neutrals arrive at and transfer energy to the substrate, thereby contributing to the thin film formation process. Note that there are also N_2^+ ions incident onto the target. However, these N_2^+ ions are first neutralized at the target surface and then react with the target metal atoms to form metal nitrides. The metal nitride has low sputter yield and the formation of metal nitride at the target surface is referred to as target poisoning. Therefore, the reflected energetic neutrals do not include N_2 molecules. The third is the incident positive ions (to the substrate), which are accelerated by the potential drop next to the substrate region (the electric sheath) and then transfer the energy to the metal nitride film. These positive ions include both Ar^+ and N_2^+.

To gain more understanding into the role of energy level in the film formation process, it is essential to quantify the incident particle fluxes (of the three types of energetic particles mentioned above) and the associated energy fluxes onto the substrate. In this study, these energetic particle fluxes and the associated energy fluxes to the substrate will be calculated at low pressure reactive sputtering conditions for TiN and TaN deposition processes.

2. METHODS

2.1. Sputtered metal atoms

The ion flux to target $F_{Ion\text{-}Tar}$ is related to the target current I_{Tar} by

$$F_{Ion\text{-}Tar} = j_{Ion\text{-}Tar} / q = I_{Ion\text{-}Tar} / (q\, A_{Tar}) \qquad (1)$$

where $j_{Ion\text{-}Tar}$ is the ion current density flowing to the target, q is the unit charge, $I_{Ion\text{-}Tar}$ is the ion current to the target, and A_{Tar} is the target area. This ion current includes contributions from both Ar^+ and N_2^+ ions. The unit for flux is number of particles per unit area per unit time, often simplified as $1/(cm^{-2}s^{-1})$.

The sputtered metal flux F_m produced by the bombarding ion flux is

$$F_m = c_m\, Y_m\, F_{Ion\text{-}Tar} \qquad (2)$$

where Y_m is the sputter yield for the target metal atoms, and c_m is a coefficient that is less than 1 and accounts for the reduction of metal sputter due to target poisoning by the nitrogen gas. This reduction is proportional to the reduction of deposition rate on the substrate, and c_m is given by

$$c_m = t/t_0 \qquad (3)$$

where t is the film thickness of the deposited metal or metal nitride film on the substrate, and t_0 is the thickness of the deposited metal film for 100% Ar gas. The values of t and t_0 are obtained from experimental measurements.

Using the analogy between the heat flux and the depositing metal flux onto a surface, the metal flux emitted from the target and then depositing onto the substrate could be computed [11]. It could be shown that

$$F_{m,Tar\text{-}Sub} = \pi\, F_m\, VF_{Tar\text{-}Sub} \qquad (4)$$

where $F_{m,Tar\text{-}Sub}$ is the depositing metal flux from the target to the substrate, and $VF_{Tar\text{-}Sub}$ is the view factor (also called the configuration factor) from the target to the substrate. $VF_{Tar\text{-}Sub}$ is given by [12]

$$VF_{Tar\text{-}Sub} = (A_{Sub} / A_{Tar})\, r^2 / (h^2 + r^2) \qquad (5)$$

where r is the target radius, and h is the distance from the target to the substrate (as shown in Figure 1), and A_{Sub} is the substrate area.

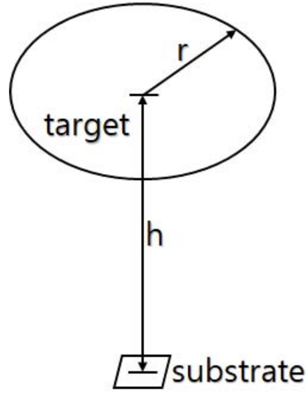

Figure 1. Geometric configurations for the target and the substrate.

The energy flux from the target to the substrate due to the sputtered metal atoms ($EF_{m,Tar\text{-}Sub}$) is

$$EF_{m,Tar\text{-}Sub} = F_{m,Tar\text{-}Sub} E_m \quad (6)$$

where E_m is the energy contribution of each metal atom (or particle) to the film formation. The value of E_m is given by

$$E_m = E_{m,ave} + U_S \quad (7)$$

where $E_{m,ave}$ is the average kinetic energy of the depositing metal atoms to the substrate, and U_S is the surface binding energy (also referred to as heat of condensation) of the metal atoms. The surface binding energies for Ti and Ta atoms are 4.86 and 8.1 eV, respectively.

2.2. Reflected energetic neutral Ar atoms

The transport of the reflected Ar atoms from the target to the substrate is similar to that of the sputtered metal atoms. It follows that

$$F_{Ar,Tar\text{-}Sub} = \pi F_{Ar} VF_{Tar\text{-}Sub} \quad (8)$$

where $F_{Ar,Tar\text{-}Sub}$ is the reflected Ar atom flux from the target to the substrate, and F_{Ar} is the reflected Ar atom flux from the target surface. F_{Ar} is given by

$$F_{Ar} = x_{Ar+} j_{Ion\text{-}Tar} / q \quad (9)$$

Here x_{Ar+} is the fraction of the incident Ar^+ ion to the target with respect to the total ion. According to a previous experimental study, the fraction of the Ar^+ ion is the same as the fraction of Ar flow rate in the total gas flow (Ar and N_2) [13]. For example, for 10 sccm Ar and 5 sccm N_2, the fraction of Ar flow rate is 0.67.

The energy flux to the substrate due the reflected Ar atoms ($EF_{Ar,Tar\text{-}Sub}$) is

$$EF_{Ar,Tar\text{-}Sub} = F_{Ar,Tar\text{-}Sub} E_{Ar} \quad (10)$$

where E_{Ar} is the energy contribution of each neutral Ar atom to the film formation. The value of E_{Ar} is given by

$$E_{Ar} = E_{Ar,ave} \quad (11)$$

where $E_{Ar,ave}$ is the average kinetic energy of the reflected Ar atoms to the substrate. The value of $E_{Ar,ave}$ is obtained through the energy-dependent thermal accommodation coefficient [9]. In this study, it is assumed that 80% of the Ar^+ ions are reflected energetically and the rest of the 20% is reflected thermally. Since N_2^+ ions react with the target metal atoms, these N_2^+ ions are not included in the reflected energetic neutrals.

2.3. Positive ions to the substrate

The positive ion flux to the substrate ($F_{Ion\text{-}Sub}$) is given by [14].

$$F_{Ion\text{-}Sub} = j_{Ion\text{-}Sub} / q = n_{Ion} (k_b T_e / m_{Ion})^{1/2} \quad (12)$$

where $j_{Ion\text{-}Sub}$ is the current density to the substrate, n_{Ion} is the total ion density that include both Ar^+ and N_2^+ ions, k_b is the Boltzmann constant, T_e is the electron temperature, and m_{Ion} is the effective ion mass.

The energy flux to the substrate due to the positive ions ($EF_{Ion\text{-}Sub}$) is

$$EF_{Ion\text{-}Sub} = F_{Ion\text{-}Sub} E_{Ion} \quad (13)$$

where E_{Ion} is the energy contribution of each positive ion to the film formation. The value of E_{Ion} is given by

$$E_{Ion} = E_{Sheath} + E_{Iz} \quad (14)$$

where E_{Sheath} is the energy gained by the ions through the electric sheath region next to the substrate, and E_{Iz} is the ionization energy of the incident ions to the substrate. The ionization energies of the Ar^+ and N_2^+ ions are 15.8 and 15.6 eV, respectively (almost identical). The value of E_{Sheath} is given by [15]:

$$E_{Sheath} = 0.5T_e + T_e \ln(m_{Ion} / m_e) \quad (15)$$

where m_e is the electron mass. The first term is the ion energy in the pre-sheath region next to the substrate, and the second term is the ion energy across the substrate sheath.

3. RESULTS AND DISCUSSION

The input values for the flux calculation are based on the experimental conditions from previous works on TiN and TaN depositions [16, 17]. The metal targets have a radius of 10 cm, and the substrate is 12 cm directly below the target (r = 10 cm and h = 12 cm in Figure 1). The substrate material is Si(100). In the flux calculations, the substrate area is set at 1 cm^2. Some experimental parameters and the calculated coefficients based on experimental results are listed in Table 1. For example, at 100% Ar the film thickness is 487 nm and at 3 sccm N_2 the film thickness is 293 nm [16]. Then the c_{Ti} at 3 sccm N_2 is 0.60 (=293/487). It turns out that at low pressure conditions (about 2 mTorr), the mean free path values of the sputtered Ti and Ta atoms are slightly larger than 12 cm [18]. Consequently, the transport process of the sputtered metal atoms from the target to the substrate can be approximated as collisionless. Hence, the average energy of the metal atoms arriving at the substrate is the same as that of the metal atoms just emitted from the target surface. For all cases, the target voltage and current values are -460 V and 0.8 A, respectively. At the target bias of -460 V, the sputter yields for Ar^+ are 0.45 and 0.40 for Ti and Ta atoms, respectively [19]. The average energies for sputtered Ti and Ta atoms due to Ar^+ ions are 20.5 and 23.7 eV, respectively [18]. Similarly, the reflected Ar neutrals also reach substrate through a collisionless transport process.

3.1. Particle energy levels

The energy levels for different particles incident onto the substrate are shown in Figure 2. The energy of the reflected Ar neutrals is 18.5 eV for all flow rates. The energies of the sputtered Ti and Ta atoms for all nitrogen flow rates are 25.4 and 31.8 eV, respectively. The energies of the Ta atoms are about 25% higher than those of the Ti atoms. The energy of the reflected Ar atoms consists of only the average energy of the reflected Ar atoms at the target surface. The energy of the sputtered metal atoms consists of the average energy of the metal atoms emitted at the target surface and the surface binding energy upon depositing onto the substrate. Both energy components are several eV higher for Ta atoms.

In Figure 2, the energy level of the Ar^+ ions are the highest, and ranges from 64.5 eV (100% Ar) to 66.1 eV (7 sccm N_2). This difference is small, only about 2.5%. The ion energy consists of the energy gained from the electric sheath and the ionization energy of the ions. As the nitrogen flow rate changes, the sheath energy also changes and this results in the changes in ion energies (for both Ar^+ and N_2^+). As the nitrogen content changes, the effective ion mass m_{Ion} in equation (14) also changes because the N_2^+ mass is only 70% that of the Ar^+ mass. Hence, the energy gained by the ions from the electric sheath ranges from 48.7 eV (100% Ar) to 50.3 eV (7 sccm N_2). The variation in sheath energy consists of the effective ion mass variation and the electron temperature variation. The electron temperature varies from 4.16 to 4.35 eV [20].

The energy level of the N_2^+ ions (not plotted) is only 0.2 eV lower than that of the Ar^+ ions.

Table 1. The values for c_m at various deposition conditions.

Case	1	2	3	4	5
N_2 (sccm)	0	3	5	7	9
Ar (sccm)	10	10	10	10	10
c_{Ti} [16]	1.0	0.60	0.31	0.27	0.25
c_{Ta} [17]	1.0	0.89	0.86	0.83	0.82

According to Equation (15), the sheath energy component value is identical for both Ar^+ and N_2^+, and the ionization energy of N_2^+ is only 0.2 eV lower than that of Ar^+. Hence, the N_2^+ energy level is not plotted here for non-zero nitrogen content. All the particle energy levels in Figure 2 are much higher than the thermal energy of the background gas atoms and molecules. For example, the thermal energy of the background Ar atoms at 300 °C is only about 0.06 eV.

3.2. Particle fluxes to the substrate

The fluxes of the sputtered Ti and Ta atoms, and the reflected Ar neutrals to the substrate are shown in Figure 3. Both the metal atom (Ti and Ta) and the Ar atom fluxes are largest at 100% Ar, and then monotonically decrease as nitrogen content increases. These decreases in the flux values are 47%, 18%, and 75% for Ar, Ta and Ti, respectively. This decrease is proportional to the fraction of the Ar flow rate for Ar atoms, and to the coefficient c_m (listed in Table 1) for Ti and Ta atoms. It is noted here that the small decrease for Ta indicates a relatively low target poisoning for Ta sputtering (as compared to Ti). For all three atoms, the magnitude of the flux is of the order of 10^{13} $cm^{-2}s^{-1}$.

The corresponding energy fluxes for the three atoms are shown in Figure 4. Since the energy flux is equal to the product of particle energy and the atom flux, the trends of the curves for the three atoms in Figure 4 match those in Figure 3. The energy fluxes for all three atoms are highest at 100% Ar. As the nitrogen content increases, the target poisoning effect also increases, and the energy fluxes for all three atoms decrease. The energy fluxes for the three atoms range from 10^{14} to 10^{15} $eVcm^{-2}s^{-1}$.

3.3. Ion fluxes to the substrate

The fluxes for Ar^+ and N_2^+ ions to the substrate are shown in Figure 5. According to Equation (12), the ion flux is proportional to ion density, and the square root of electron temperature and the inverse of ion mass. The ion density is the

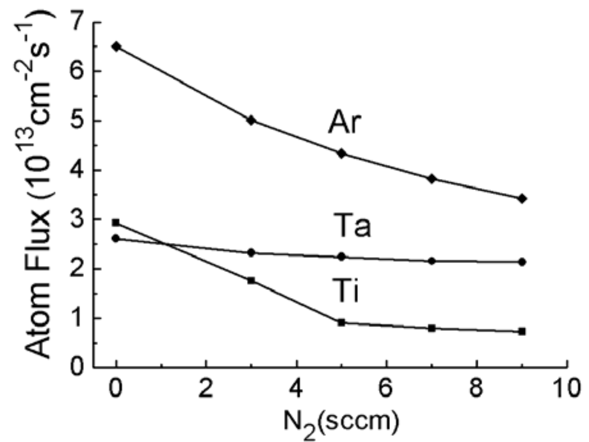

Figure 3. Fluxes for sputtered Ti and Ta atoms, and reflected Ar neutrals to the substrate.

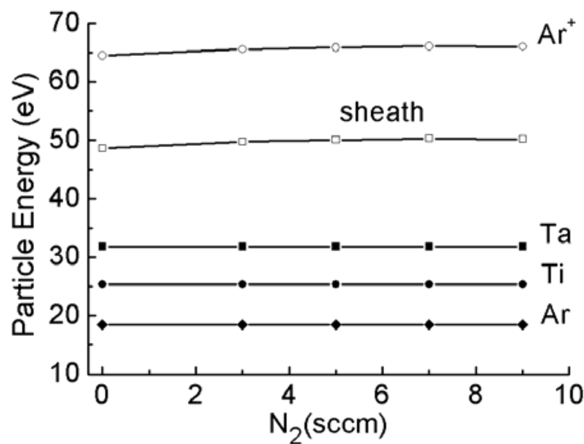

Figure 2. Energy levels for sputtered metal atoms, reflected Ar neutrals, and Ar^+ ions to the substrate.

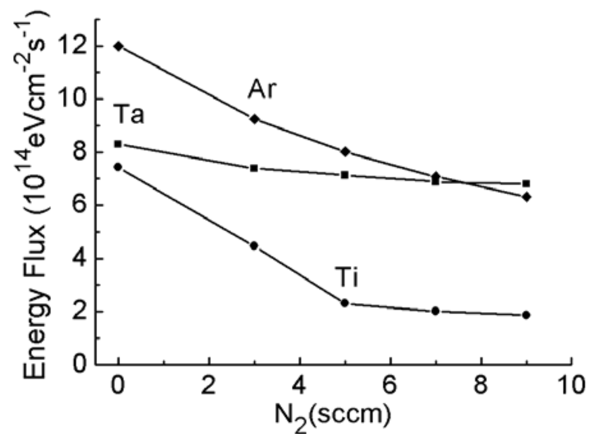

Figure 4. Energy fluxes for sputtered Ti and Ta atoms, and reflected Ar neutrals to the substrate.

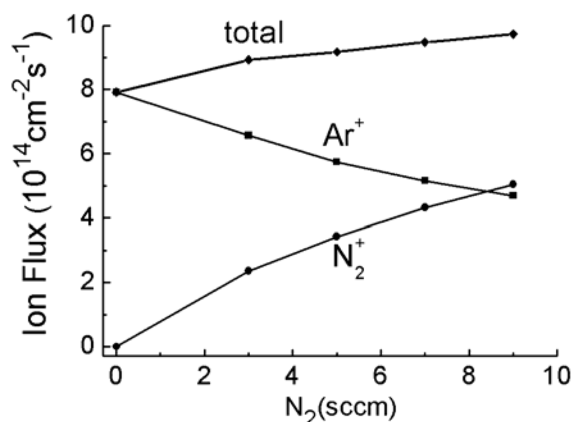

Figure 5. Fluxes for Ar^+ and N_2^+ ions to the substrate.

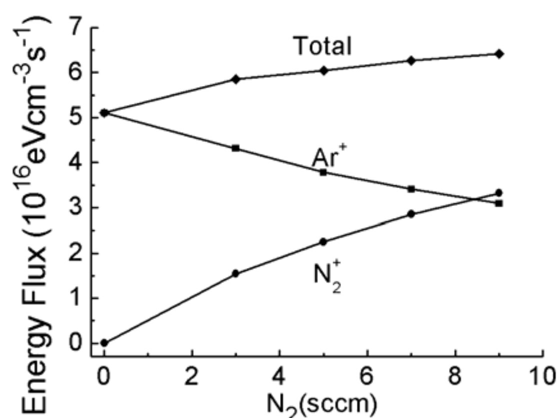

Figure 6. Energy fluxes for Ar^+ and N_2^+ ions to the substrate.

primary influence on the ion flux density, while the ion mass is secondary. As previously mentioned, the electron temperature variation is small. As the percentage of Ar decreases and that of N_2 increases, the Ar^+ flux decreases and the N_2^+ flux increases, as expected. Note that at 10 sccm Ar and 9 sccm N_2, the N_2^+ flux is slightly higher than the Ar^+ flux due to the difference in ion mass between the Ar^+ and the N_2^+ ions. The total ion flux increases from 7.9 to 9.7×10^{14} $cm^{-2}s^{-1}$ as the N_2 flow increases. The total ion flux is about ten times that of the total atoms fluxes (Ar plus Ti or Ar plus Ta). This is due to the acceleration of the ions by the electric sheath adjacent to the substrate.

The energy fluxes for Ar^+ and N_2^+ ions to the substrate are shown in Figure 6. The trends for the ion energy fluxes are the same as those for the ion fluxes in Figure 5. The total ion energy flux ranges from 5.1 to 6.4×10^{16} $eVcm^{-2}s^{-1}$. The total ion energy flux is about 25 to 50 times that of the total atom energy fluxes (Ar plus Ti or Ar plus Ta). This is due to the larger magnitude for both the ion flux and the ion energy compared to the neutral atom flux and energy. This dominance of the ion energy flux indicates that the ions in plasma could supply a large amount of energy during the thin film formation process even for a moderate ion density of about 2.7×10^9 cm^{-3}. This large ion energy flux is much higher than the energy flux associated with the energetic neutrals (sputtered Ti, Ta atoms and the reflected Ar atoms) unique to the sputter process. The combined energy contributions from the ions and the energetic neutrals are beneficial to the quality of the deposited thin films.

4. CONCLUSIONS

This study computed the energy associated with the sputter metal atoms (Ti and Ta), the Ar neutral atoms that are reflected from the target, and the incident Ar^+ and N_2^+ ions to the substrate under low pressure conditions (about 2 mTorr) during reactive sputtering. Moreover, the corresponding particle and energy fluxes to the substrate are also calculated. The calculated values indicate that the energy levels for both atoms and ions are elevated during the sputtering process, and the ion energy levels (above 60 eV) are higher than the energy level of the neutrals (about 20 to 30 eV). In addition, the total ion flux to the substrate is about 10 times that of the neutral flux. Consequently, the total ion energy flux to the substrate is dominant (25 to 50 times) over the total neutral energy flux.

CONFLICT OF INTEREST STATEMENT

There are no conflicts of interests.

REFERENCES

1. Saoula, N., Djerourou, S., Yahiaoui, K., Henda, K., Kesri, R., Erasmus, R. M. and Comins, J. D. 2010, Surf. Interface Anal., 42, 1176.

2. Kim, S. H., Park, H., Lee, K. H., Jee, S. H., Kim, D. J., Yoon, Y. S. and Chae, H. B. 2009, J. Ceram. Process. Res., 10, 49.
3. Qu, X. P., Tan, J. J., Zhou, M., Chen, T., Xie, Q., Ru, G. P. and Li, B. Z. 2006, Appl. Phys. Lett., 88, 151912.
4. Lu, J. and Arshi, N. 2016, JOM, 68, 1634.
5. Patsalas, P., Charitidis, C. and Logothetidis, S. 2000, Surf. Coat. Technol., 125, 335.
6. Kim, S. K. and Cha, B. C. 2005, Thin Solid Films, 475, 202.
7. Serikov, V. V. and Nanbu, K. 1997, J. Appl. Phys., 82, 5948.
8. Kersch, A., Morokoff, W. and Werner, C. 1994, J. Appl. Phys., 75, 2278.
9. Lu, J. and Kushner, M. J. 2000, J. Appl. Phys., 87, 7198.
10. Lu, J. and Lee, C. G. 2012, Vacuum, 86, 1134.
11. Lu, J., Yoon, J. H., Cho, T. Y., Joo, Y. K. and Lee C. G. 2007, Met. Mater. Int., 13, 123.
12. Siegel, R. and Howell, J. R. 1992, Thermal Radiation Heat Transfer, Taylor & Francis, Washington DC.
13. Petrov, I., Myers, A., Greene, J. E. and Abelson, J. R. 1994, J. Vac. Sci. Technol., 12, 2846.
14. Lu, J., Krier, H., Burton, R. L. and Goodfellow, K. D. 1998, J. Thermophys. Heat Transfer, 12, 230.
15. Liebermann, M. A. and Lichtenberg, A. J. 2005, Principles of Plasma Discharges and Materials Processing, Wiley, New York City.
16. Arshi, N., Lu, J., Joo, Y. K., Lee, C. G., Yoon, J. H. and Ahmed, F. 2013, Mater. Sci.: Mater. Electron., 24, 1194.
17. Arshi, N., Lu, J., Joo, Y. K., Yoon, J. H. and Koo, B. K. 2015, Surf. Interface Anal., 47, 154.
18. Lu, J. 2018, AIP Conference Proceedings, 2043, 020001.
19. Yamamura, Y. and Tawara, H. 1996, At. Data Nucl. Data Tables, 62, 149.
20. Lu, J. 2020, AIP Conference Proceedings, 2221, 060002.